Article ID: 1000-324X(2022)12-1365-06 **DOI:** 10.15541/jim20220162

High Piezoelectric Property and Low Electric Field-strain Hysteresis of $BiAlO_3$-doped PZT Ceramics

LIU Dingwei[1,2], ZENG Jiangtao[1], ZHENG Liaoying[1], MAN Zhenyong[1], RUAN Xuezheng[1], SHI Xue[1], LI Guorong[1]

(1. Key Laboratory of Inorganic Functional Material and Device, Shanghai Institute of Ceramics, Chinese Academy of Sciences, Shanghai 200050, China; 2. Center of Materials Science and Optoelectronics Engineering, University of Chinese Academy of Sciences, Beijing 100049, China)

Abstract: Lead-based piezoelectric ceramics are widely used in piezoelectric devices due to their excellent piezoelectric properties. Piezoelectric actuators require piezoelectric ceramics with high piezoelectric properties and high precision displacement as well as small strain hysteresis under applied electric fields, which can be obtained by donor-acceptor co-doping. In this work, $(1–x)(Pb_{0.95}Sr_{0.05})(Zr_{53}Ti_{47})O_3$-$xBiAlO_3$ + 0.2%MnO_2 ceramics were prepared by a traditional solid-state reaction method (doping amount in mass percentage). The microstructure and piezoelectric properties of the prepared ceramics were investigated. The results demonstrated that the defect dipole can hinder the domain rotation in a few additions of $BiAlO_3$, resulting in a relatively low piezoelectric property and low strain hysteresis under electric fields. With more $BiAlO_3$ addition, the piezoelectric properties and strain hysteresis of the ceramics are improved because the pinning effect to the domain rotation become weak. The optimal performance is obtained at x=1.75%, where the piezoelectric coefficient (d_{33}), electromechanical coupling coefficient (k_p), mechanical quality factor (Q_m) and Curie temperature (T_C) are 504 pC/N, 0.71, 281 and 312 ℃, respectively. This piezoelectric ceramic show a relative high strain and low strain hysteresis (only 15%) under the electric field of 10 kV/cm. Due to the high piezoelectric performance and low electric field strain hysteresis along with the good temperature stability, the $(1–x)(Pb_{0.95}Sr_{0.05})(Zr_{53}Ti_{47})O_3$-$xBiAlO_3$ + 0.2%MnO_2 ceramics can be a kind of piezoelectric ceramic with practical application potentials for the piezoelectric actuators.

Key words: piezoelectric properties; low strain hysteresis; temperature stability; PZT; $BiAlO_3$ doping

Lead-based piezoelectric ceramics play a significant role in the application of piezoelectric devices, owing to their excellent ferroelectric and piezoelectric properties[1-3]. For piezoelectric actuators, the high electric field-induced strain and the low hysteresis are required[4]. Relaxor ferroelectrics with the nano-domain or polar nano-region (PNR) are potential to meet this need because the nano-domains or PNR are ready to rotate to the direction of the applied electric fields, and they are reversible to their original state as the applied field to be zero[5]. Nevertheless, due to the low ferroelectric-paraelectric phase transition temperature and narrow temperature range, the practical applications of relaxor ferroelectric are significantly limited[6]. Comparison with relaxor ferroelectric, PZT-based ceramics have higher phase transition temperatures, making it possible to work at higher temperatures. Due to the better electric-field induced strain behaviors and excellent temperature stability, PZT materials have been irreplaceable in the field of actuators so far.

To obtain a high electric-field induced strain with a low hysteresis in PZT-based ceramics, doping elements is one of the most effective methods. Nowadays, researchers have mainly focused on co-doping[7] to optimize the piezoelectric properties of piezoelectric ceramics. Yan, *et al*[8] studied the property of Li^+ and Bi^{3+} co-doped

Received date: 2022-03-22; **Revised date:** 2022-07-06; **Published online:** 2022-08-26
Foundation item: National Natural Science Foundation of China (51831010); National Key R&D Program (2021YFA0716502, 2021YFB3800604)
Biography: LIU Dingwei (1998–), male, Master candidate. E-mail: liudingwei@student.sic.ac.cn
刘鼎伟(1998–), 男, 硕士研究生. E-mail: liudingwei@student.sic.ac.cn
Corresponding author: LI Guorong, professor. E-mail: grli@mail.sic.ac.cn
李国荣, 研究员. E-mail: grli@mail.sic.ac.cn

$PbHf_{0.3}Ti_{0.7}$-$PbNb_{2/3}Ni_{1/3}$ piezoelectric ceramics with d_{33} of higher than 1000 pC/N but Curie temperature of only 120 ℃. Feng, *et al*[9] investigated the Li^+ and Al^{3+} co-doped PZT ceramics and obtained the optimal property with d_{33}=310 pC/N, k_p=0.5, which also performed excellent temperature stability. Nevertheless, synergic optimization of the piezoelectric constant, the temperature stability, and *S-E* loops hysteresis property of piezoelectric ceramics have been rarely investigated.

In this work, $BiAlO_3$ was introduced into PZT ceramics to obtain high performances in piezoelectric properties and *S-E* hysteresis loops. In these ceramics, A-site of Pb^{2+} was replaced by a higher valence cation of Bi^{3+} and B-site of Zr^{4+} or Ti^{4+} was replaced by a lower valence cation of Al^{3+}. Donor doping makes ceramics possess a large strain[10] and acceptor doping makes ceramics possess a small electric field induced strain hysteresis[11]. Meanwhile, Mn[12] and Sr[13] were introduced for good piezoelectric ceramics with high piezoelectric properties, low *S-E* hysteresis loops, and great temperature stability.

1 Experimental

$BiAlO_3$ doped $(Pb,Sr)(Zr,Ti)O_3$ with $0.2\%MnO_2((1–x)(Pb_{0.95}Sr_{0.05})(Zr_{0.53}Ti_{0.47})O_3$-$xBiAlO_3$+ $0.2\%MnO_2$, MnO_2 doping amount in mass fraction, x=0.50%, 0.75%, 1.00%, 1.25%, 1.50%, 1.75%, 2.00%, and 2.25%, in mol fraction) ceramics, hereinafter abbreviated as (1–*x*)PSZT-*x*BA-0.2Mn, were prepared by a traditional solid-state reaction. The raw materials PbO(99.9%), $SrCO_3$(99%), ZrO_2(99.9%), TiO_2(99.7%), Bi_2O_3(99.6%), Al_2O_3(99.99%), and MnO_2(99.99%) were weighted stoichiometrically and mixed for 10 h using a ball milling with water. Then the mixed powders were calcined at 820 ℃ for 2 h. The calcined powders were ball-milled and dried again to obtain homogeneous powders. The obtained powders were mixed with the polyvinyl alcohol as binder and pressed into disks (ϕ12 mm×1 mm) under a uniaxial pressure of 200 MPa. The disks were burned at 550 ℃ for 3 h to remove the binder. After burning out the binder, the disks were sintered in air at 1160 ℃ for 2 h. Silver electrodes were coated on top and bottom surfaces of the ceramics and burned at 720 ℃ for 30 min. For piezoelectric properties measurements, ceramics were poled under 40 kV/cm at 120 ℃ for 30 min.

The lattice structure of the sintered samples was measured by X-ray diffraction analysis with CuKα radiation (DX-2700BH, Haoyuan, China). Scanning electron microscope (Phenom Pure-SED G6, China) was used to observe the grain size. The polarization-electric field (*P-E*) and the strain-electric field (*S-E*) hysteresis loops of samples were measured with a TF analyzer (TF Analyzer 2000E, aixACCT Systems GmbH, Aachen, Germany). The piezoelectric constant d_{33} was measured by a quasistatic piezoelectric d_{33} meter (ZJ-3A, China Academy of Acoustics, China). The dielectric constant (ε_r) and dielectric loss (tanδ) were measured by an impedance analyzer (Agilent 4294A, Agilent Technologies, Japan). The electromechanical coupling factor (k_p) and mechanical quality factor (Q_m) were calculated using the resonance and anti-resonance method with the impedance analyzer.

2 Results and discussions

XRD patterns of (1–*x*)PSZT-*x*BA-0.2Mn ceramics are shown in Fig. 1(a). The results show that ceramics with all compositions contain pure perovskite structures within the detection resolution limitation. To show the evolution of phase structure clearly, the enlarged XRD patterns of (200) peak between 43°–46° of 2θ are shown in Fig. 1(b). All peaks near 2θ=44.5° can be separated into three peaks by Gaussian fitting. Two of the peaks correspond to the tetragonal phase ((200), (002)), and the third one corresponds to the rhombohedral phase (020). However, it is clear that the coexistence of the rhombohedral and the tetragonal phases occurs in all ceramics. Thus, the ceramics with compositions x=0.50% to x=2.25% are identified as located in the morphotropic phase boundary (MPB) for this system[14].

Fig. 2 shows the evolution of grain microscopic images of SEM for $BiAlO_3$ doping (1–*x*)PSZT-*x*BA-0.2Mn ceramics of some doping contents. Since SEM images for all compositions are quite similar, four representative compositions are selected from all compositions. The black points in grains and at grain boundaries in SEM are considered pores. The grain sizes of (1–*x*)PSZT-*x*BA-0.2Mn ceramics were calculated by a statistical method. With the doping of $BiAlO_3$, the average size of grain increases

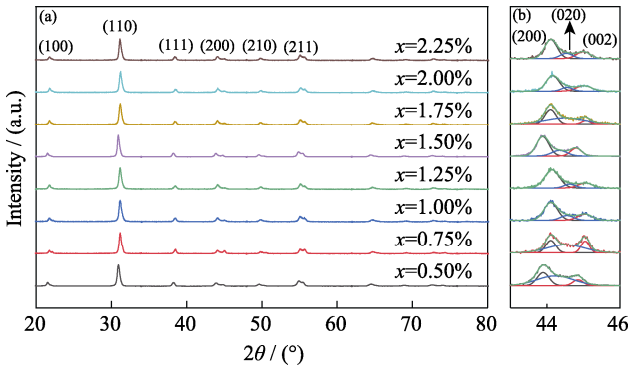

Fig. 1 XRD patterns of (1–*x*)PSZT-*x*BA-0.2Mn ceramics
(a) 20°–80°; (b) Near (200) peak

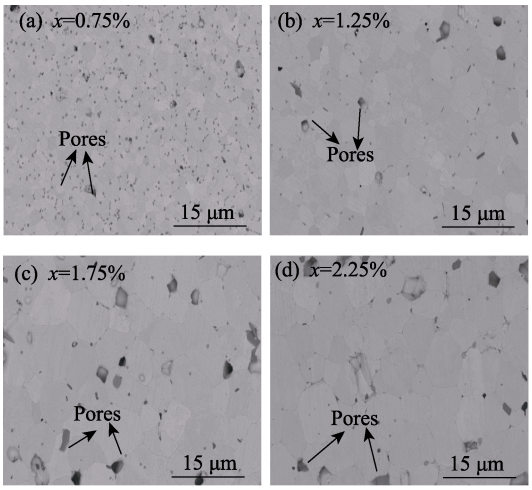

Fig. 2 SEM images for surface microstructures of (1–*x*)PSZT-*x*BA-0.2Mn ceramics

firstly and then decreases, from 1.6 μm (*x*=0.50%) to 6.7 μm (*x*=2.00%) and then to 6.2 μm (*x*=2.25%). The average grain size reaches maximum at *x*=2.00%, indicating that a suitable amount of $BiAlO_3$ can benefit grain growth. Because Bi^{3+} can be used to reduce the sintering temperature[15], lower sintering temperatures of about 1160 ℃ are required with the increasing of the content of Bi^{3+}, resulting in many small pores in ceramics with *x*=0.75% and a few large pores in ceramics with *x*=2.25%.

The temperature-dependent dielectric constant (ε_r) and dielectric loss (tanδ) at different frequencies of (1–*x*)PSZT-*x*BA-0.2Mn (*x*=0.75%, 1.25%, 1.75%, and 2.25%, in mol fraction) ceramics are shown in Fig. 3. It is found that the temperature of maximum ε_r for each frequency has no apparent changes with frequency, indicating that they are normal ferroelectric rather than relaxor ferroelectric ceramics. The temperature of maximum ε_r for this kind of ceramics is Curie temperature[16]. It is observed that T_C varies from 310 ℃ to 320 ℃, indicating that the operating temperature range of ceramics is wider. In addition, the dielectric curves have a broad Curie peak, indicating the existence of the diffused phase transition (DPT)[17]. The existence of the DPT suggests that there exists a microdomain structure that affects the piezoelectric properties of ceramics[18].

P-E loops, *I-E* loops and *S-E* loops of (1–*x*)PSZT-*x*BA-0.2Mn measured at a maximum electric field of 40 kV/cm and the frequency of 10 Hz are shown in Fig. 4. It can be seen that (1–*x*)PSZT-*x*BA-0.2Mn ceramics with $x \leqslant 1.00\%$ show the pinched *P-E* loops. With the further increase of BA content, the *P-E* loops become normal and the remnant polarization increases abruptly. The pinched *P-E* loops should not be attributed to the antiferroelectric phase of $PbZrO_3$ because all ceramics are located in the MPB. Hence, the phenomenon is mainly attributed to the fact that a part of the domains is hard to reverse along the direction of the applied electric field[15]. Mn ion plays a significant role as an acceptor doping instead of the B-site of Ti^{4+} ions (Mn''_{Ti}), Mn''_{Ti} and $V_O^{\cdot\cdot}$ form (Mn''_{Ti} - $V_O^{\cdot\cdot}$) defect dipoles. Considering the pinning effect of defect dipoles, it is believed that the domains in PZT ceramics are pinned by defect dipoles, which made the rotation of domains more difficult and revert to the initial state quickly after removing the electric field[19]. The defect dipoles also resulted in a small P_r of the ceramics.

When the content of $BiAlO_3$ is low, the content of Al^{3+} in these ceramics is similar to that of Mn^{2+}, and Al ion plays an important role as well as Mn in the unsaturated shape loops. With the increasing of $BiAlO_3$ content, $BiAlO_3$ has a stronger effect on the properties of ceramics. Like $(Mn''_{Ti} - V_O^{\cdot\cdot})$ dipoles, $(Al'_{Ti} - V_O^{\cdot\cdot})$ charged dipoles are formed by Al'_{Ti} and $V_O^{\cdot\cdot}$. However, the pinning effect of $(Al'_{Ti} - V_O^{\cdot\cdot})$ charged dipoles are weaker than $(Mn''_{Ti} - V_O^{\cdot\cdot})$ dipoles and more domains rotate under electric field. Meanwhile, Bi^{3+} replaces the site of Pb^{2+} as a donor doping, which leads to the perovskite lattice distortion and domains easily rotate. Eventually, with the increase of $BiAlO_3$ content, domains can rotate easily. Besides, the unsaturated *P-E* loops become standard with the addition of $BiAlO_3$, indicating that the defect dipoles in (1–*x*)PSZT-*x*BA-0.2Mn ceramics could rotate easily.

The same results can be found in *I-E* loops, as shown in Fig. 4(b). The appearance of the current peaks indicates the existence of domain rotation under electric fields, and the intensity of the peaks represents the strength of the domain rotation. There are four peaks separately caused by the motion of defect dipoles and domain switching in ceramics with compositions of low content, indicating the existence of defect dipoles in ceramics[20]. However, only two peaks caused by the domain switching can be observed as the content of $BiAlO_3$ increasing from *x*=1.50%. The intensity of the current peaks increases gradually, indicating that more domains are switched and suggesting better piezoelectric properties. The results show that the $BiAlO_3$ makes ceramics behave like soft-doped ceramics.

It also can be confirmed from the *S-E* loops, as shown in Fig. 4(c). The *S-E* loops exhibit the characteristic of butterfly shape, and the negative strain increases with the increase of $BiAlO_3$ content. This is because the weaker

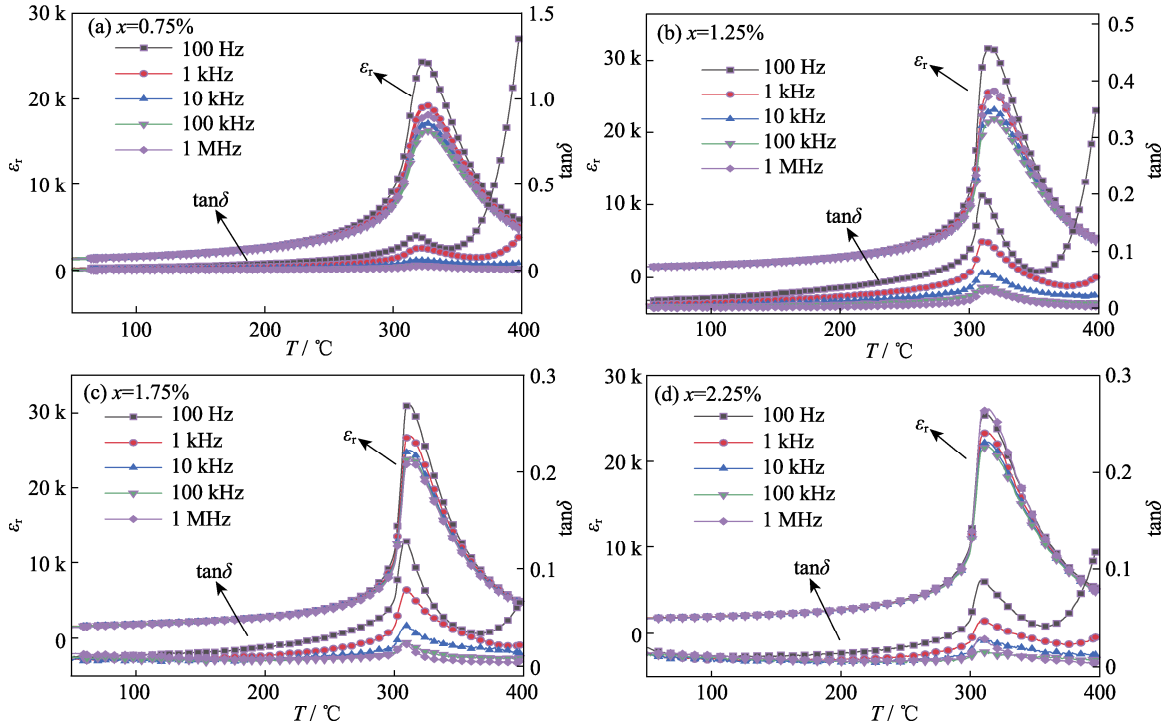

Fig. 3 Temperature dependent dielectric constant (ε_r) and dielectric loss (tanδ) of (1–x)PSZT-xBA-0.2Mn (x=0.75%, 1.25%, 1.75%, and 2.25%, in mol fraction) at different frequencies

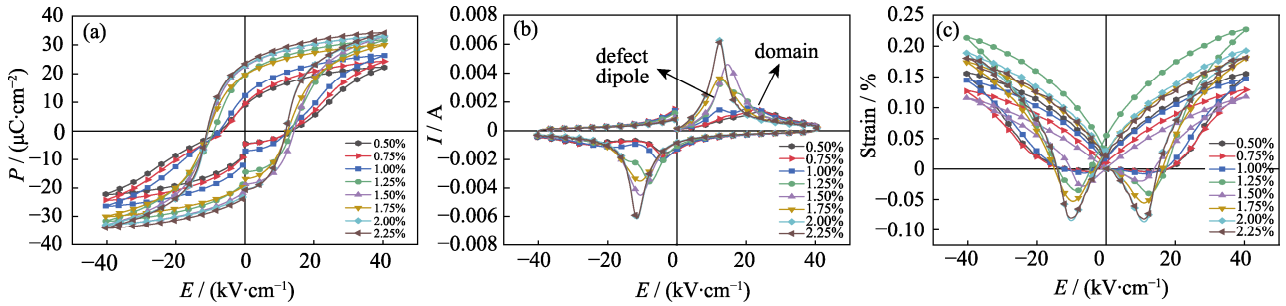

Fig. 4 Ferroelectric properties of the (1–x)PSZT-xBA-0.2Mn ceramics (x=0.50%, 0.75%, 1.00%, 1.25%, 1.50%, 1.75%, 2.00%, and 2.25%, in mol fraction)
(a) Polarization-electric field (P-E) hysteresis loops; (b) Current-electric field (I-E) loops; (c) Strain-electric field (S-E) loops (40kV/cm, 10Hz)

pinning effect of defect dipoles make the rotation of domain easier under electric field as the $BiAlO_3$ content increases.

The piezoelectric and dielectric properties of (1–x)PSZT-xBA-0.2Mn ceramics are shown in Table 1. It can be seen that the k_p, d_{33}, and Q_m increase firstly and then decrease with the increase of $BiAlO_3$ content. The dielectric constant and loss maintain steadily at first and then increase rapidly. Here, higher piezoelectric constant is attributed to the phase structure of MPB and fewer domains affected by defect dipoles. With the increase of $BiAlO_3$ content, the ceramics perform a characteristic like soft piezoelectric ceramics with a lower Q_m and higher tanδ. The optimum property are found at the composition of x=1.75%, with k_p=0.71, d_{33}=504 pC/N, Q_m=281, tanδ=0.26%, ε_r =1470, which shows that it has better performance than commercial piezoelectric ceramic PZT-4 (k_p=0.58, d_{33}=289 pC/N, tanδ=0.4%).

For piezoelectric actuators, high field effective piezoelectric coefficient d_{33}^* and strain hysteresis H are used to describe electric field induce strain properties. d_{33}^* and H could be calculated by the following equations (1-2):

$$d_{33}^* = S_{max}/E_{max} \quad (1)$$

$$H = \Delta S_{E_{max/2}}/S_{max} \quad (2)$$

where E_{max} is the maximum electric field and S_{max} is the maximum strain, while $\Delta S_{E_{max/2}}$ is the difference in strain when rising and lowing the electric fields at half maximum electric field $E_{max/2}$.

The characterizations of the unipolar strain loops of

表 1　各组分陶瓷性能参数

Table 1　Performance parameters of different component ceramics

(1–*x*)PSZT-*x*BA-0.2Mn/ (%, in mol fraction)	Average strain size/μm	d_{33}/(pC·N^{-1})	k_p	Q_m	T_C/℃	ε	tanδ/%	d_{33}^* /(pC·N^{-1})	H/%
0.50	1.6	333	0.68	992	329	1290	0.22	380	10
0.75	1.9	367	0.69	1131	324	1300	0.27	398	8
1.00	2.5	383	0.70	827	318	1293	0.32	407	3
1.25	3.0	402	0.73	853	316	1420	0.30	540	12
1.50	4.5	460	0.72	445	311	1416	0.32	538	12
1.75	6.3	504	0.71	281	312	1470	0.27	699	15
2.00	6.7	532	0.73	130	310	1690	0.66	638	13
2.25	6.2	501	0.69	113	312	1669	1.01	710	17

(1–*x*)PSZT-*x*BA-0.2Mn measured at the electric field of 10 kV/cm with the frequency of 10 Hz are shown in Fig. 5. With the doping of $BiAlO_3$, the d_{33}^* increases from 380 pC/N (x=0.50%) to 710 pC/N (x=2.25%) and the H increases from 10% (x=0.50%) to 17% (x=2.25%). Thus, the optimum properties are found in the MPB composition at x=1.75%, with H=15% and d_{33}^* = 699 pC/N. The composition at x=1.75% possesses a high electric-field induced strain and has the advantages of small dielectric loss and small strain hysteresis, making it as an excellent material for piezoelectric actuators[21].

Temperature characteristics of unipolar strain loops of the x=1.75% composition measured at the electric field of 30 kV/cm and the frequency of 10 Hz are shown in Fig. 6. It is found that the value of d_{33}^* increases at first and then decreases with the temperature increasing. However, d_{33}^* changes slightly from ~725 pC/N to ~755 pC/N with the increase of temperature and the rate of temperature change is only 4%. The phenomenon is attributed to high T_C which is up to 312 ℃. This result suggests that the temperature stability of these ceramics is excellent.

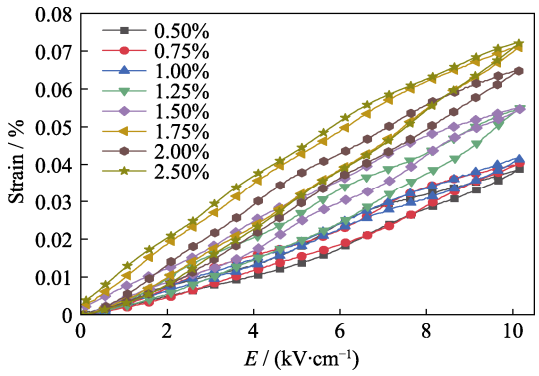

Fig. 5 Unipolar strains-electric (*S*-*E*) fields of (1–*x*)PSZT-*x*BA-0.2Mn (x=0.50%–2.25%)

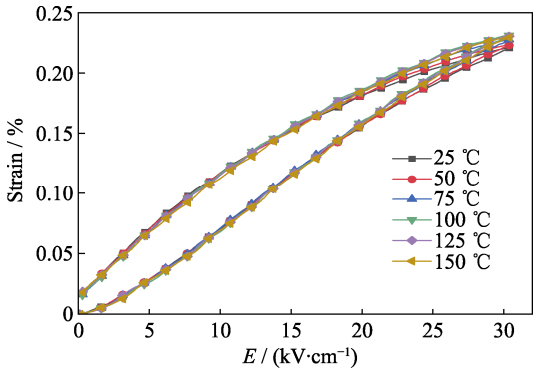

Fig. 6 Unipolar strains-electric (*S*-*E*) fields of (1–*x*)PSZT-*x*BA-0.2Mn ceramics (x=1.75%) (30kV/cm, 10Hz)

3　Conclusion

$BiAlO_3$ doped PZT ceramics with the composition (1–*x*)($Pb_{0.95}Sr_{0.05}$)($Ti_{0.53}Zr_{0.47}$)O_3-*x*$BiAlO_3$-0.2Mn near the morphotropic phase boundary (MPB) structure show excellent high piezoelectric properties and low electric field-strain hysteresis. All ceramics showed pure perovskite structures and they are identified as located in the morphotropic phase boundary (MPB) of this system. In these ceramics, the $(Mn''_{Ti} - V_O^{\cdot\cdot})$ defect dipoles hinder the domain rotation under electric field and the rotated domains revert to the initial state quickly after removing the electric field. With the increase of $BiAlO_3$ content, there would be more Bi^{3+} to promote domain rotation, which causes the ceramics exhibit higher piezoelectric properties (k_p and d_{33}). The best strain performance is achieved at x=1.75%, in which the relative strain reaches 0.07%, and the hysteresis is only 15% at 10 kV/cm. Meanwhile, the ceramic has good temperature stability, which is attributed to the high Curie temperature of the ceramic. Our results show that the ceramics at x=1.75% can be used as a piezoelectric actuator, which has the performance of high piezoelectric

properties and low electric field- strain hysteresis.

References:

[1] CROSS L E. Ferroelectric materials for electromechanical transducer applications. *Materials Chemistry and Physics*, 1996, **43:** 108–115.

[2] CHAN H I W. Smart Ferroelectric materials for sensors and mechatronic device applications. Proceedings 1999 IEEE Hong Kong Electron Devices Meeting (HKEDM 99). Hong Kong, 1999**:** 68–71.

[3] KHOLKIN A L, BDIKIN I K, KISELEV D A, *et al.* Nanoscale characterization of polycrystalline ferroelectric materials for piezoelectric applications. *Journal of Electroceramics*, 2007, **19:** 83–96.

[4] PARK S E, SHROUT T R. Ultrahigh strain and piezoelectric behavior in relaxor based ferroelectric single crystals. *Journal of Applied Physics*, 1997, **82:** 1804–1811.

[5] DONG C, LIANG R H, ZHOU Z Y, *et al.* Piezoelectric property of PZT-based relaxor-ferroelectric ceramics enhanced by Sm doping. *Journal of Inorganic Materials*, 2021, **36:** 1270–1276.

[6] LIU X, XUE S D, MA J P, *et al.* Electric-field-induced local distortion and large electrostrictive effects in lead-free NBT-based relaxor ferroelectrics. *Journal of the European Ceramic Society*, 2018, **38:** 4631–4639.

[7] PENG J G L, ZENG J T, LI G R, *et al.* Softening-hardening transition of electrical properties for Fe^{3+}-doped $(Pb_{0.94}Sr_{0.05}La_{0.01})$-$(Zr_{0.53}Ti_{0.47})O_3$ piezoelectric ceramics. *Ceramics International*, 2017, **43:** 13233–13239.

[8] YAN Y X, LI Z M, XIA Y S, *et al.* Ultra-high piezoelectric and dielectric properties of low-temperature-sintered lead hafnium titanate-lead niobium nickelate ceramics. *Ceramics International*, 2020, **46:** 5448–5453.

[9] FENG Y, LI W L, XU D, *et al.* Enhanced piezoelectric properties and constricted hysteresis behaviour in PZT ceramics induced by Li^+-Al^{3+} ionic pairs. *RSC Advances*, 2016, **6:** 36118–36124.

[10] THONGMEE N, WATCHARAPASORN A, JIANSIRISOMBOONS. Structure-property relations of ferroelectric $Pb(Zr_{0.52}Ti_{0.48})O_3$-$(Bi_{3.25}La_{0.75})Ti_3O_{12}$ ceramics. *Current Applied Physics*, 2008, **8:** 367–371.

[11] KIM Y M, KIM J C, UR S C, *et al.* Effects of Al_2O_3 on the piezoelectric properties of $Pb(Mn_{1/3}Nb_{2/3})O_3$-$PbZrO_3$-$PbTiO_3$ ceramics. *Journal of Electroceramics*, 2006, **16:** 347–350.

[12] LEE S M, LEE S H, YOON C B, *et al.* Low-temperature sintering of MnO_2-doped PZT-PZN piezoelectric ceramics. *Journal of Electroceramics*, 2007, **18:** 311–315.

[13] KOZIELSKI L, ADAMCZYK M, ERHART J, *et al.* Application testing of Sr doping effect of PZT ceramics on the piezoelectric transformer gain and efficiency proposed for MEMS actuators driving. *Journal of Electroceramics*, 2012, **29:** 133–138.

[14] PANDEY D, SINGH A K, BAIK S. Stability of ferroic phases in the highly piezoelectric $Pb(Zr_xTi_{1-x})O_3$ ceramics. *Acta Crystallographica A-Foundation and Advances*, 2008, **64:** 192–203.

[15] KIM H T, NAM M H, KIM J H, *et al.* Microwave dielectric properties and chemical resistance of low-temperature-sintered $CaZrB_2O_6$ ceramics. *International Journal of Applied Ceramic Technology*, 2009, **6:** 587–592.

[16] KUZENKO D V. Critical temperature below the Curie temperature of ferroelectric ceramics PZT. *Journal of Advanced Dielectrics*, 2021, **11:** 2150006.

[17] PEREIRA M, PEIXOTO A G, GOMES M J M. Effect of Nb doping on the microstructural and electrical properties of the PZT ceramics. *Journal of the European Ceramic Society*, 2001, **21:** 1353–1356.

[18] SHUKLA A K, AGRAWAL V K, DAS I M L, *et al.* Dielectric response of PLZT ceramics *x*/57/43 across ferroelectric-paraelectric phase transition. *Bull. Mat. Sci.*, 2011, **34:** 133–142.

[19] KAMEL T M, DE WITH G. Poling of hard ferroelectric PZT ceramics. *Journal of the European Ceramic Society*, 2008, **28:** 1827–1838.

[20] REN X B. Large electric-field-induced strain in ferroelectric crystals by point-defect-mediated reversible domain switching. *Nature Materials*, 2004, **3:** 91–94.

[21] LI F, ZHANG S J, LI Z R, *et al.* Recent development on relaxor-$PbTiO_3$ single crystals: the origin of high piezoelectric response. *Progress in Physics*, 2012, **32:** 178–198.

$BiAlO_3$ 掺杂 PZT 陶瓷的高压电性能和低电场应变滞后

刘鼎伟[1,2], 曾江涛[1], 郑嘹赢[1], 满振勇[1], 阮学政[1], 时 雪[1], 李国荣[1]

(1. 中国科学院 上海硅酸盐研究所, 无机功能材料与器件重点实验室, 上海 200050; 2. 中国科学院大学 材料科学与光电子工程中心, 北京 100049)

摘 要: 铅基压电陶瓷因其优异的压电性能, 被广泛应用于压电器件。其中, 压电驱动器要求压电陶瓷具有较高压电性能并且在电场下具有较高的电致应变和较小的应变滞后。本研究通过施主–受主共掺, 得到高压电性能和低电场应变滞后的 PZT 陶瓷。采用传统固相反应法制备了$(1–x)(Pb_{0.95}Sr_{0.05})(Zr_{53}Ti_{47})O_3$-$xBiAlO_3$+0.2%$MnO_2$ 陶瓷(掺杂量为质量百分数), 并对其微观结构和压电性能进行了研究。结果表明: $BiAlO_3$ 掺杂量较少时, 陶瓷中缺陷偶极子的“钉扎”效应使得陶瓷畴壁转动困难, 陶瓷压电性能较弱, 应变滞后也较小。随 $BiAlO_3$ 掺杂量增加, 缺陷偶极子“钉扎”效应减弱, 陶瓷的压电性能和应变滞后随之提高。本实验得到的性能最优组分为 x=1.75%, 该组份陶瓷的压电系数 d_{33}=504 pC/N, 机电耦合系数 k_p=0.71, 机械品质因数 Q_m=281, 居里温度 T_C=312 ℃, 在 10 kV/cm 电场下的应变滞后仅为 15%, 并且还具有较好的温度稳定性, 是一种具有应用价值的压电驱动器用压电陶瓷材料。

关 键 词: 压电性能; 低应变滞后; 温度稳定性; PZT; $BiAlO_3$ 掺杂

中图分类号: TQ174 **文献标志码**: A